

## Noise Equivalent Temperature Difference Model for Thermal Imagers, Calculation and Analysis

Anis Redjimi<sup>1)</sup>  
 Dragan Knežević<sup>2)</sup>  
 Katarina Savić<sup>2)</sup>  
 Nikola Jovanović<sup>2)</sup>  
 Marina Simović<sup>3)</sup>  
 Darko Vasiljević<sup>4)</sup>

Noise equivalent temperature difference (NETD) or thermal sensitivity is considered to be of great importance for the process of evaluating and comparing performances of thermal imagers which are essentially non-contact temperature measurement devices. This paper describes an NETD calculation application based on the detector specific detectivity. The NETD for several types of thermal imagers was estimated and compared with the declared values provided by the producers. The mathematical model used in this process is strongly dependent on the specific detectivity of the detector. For this reason, a number of geometrical curves are introduced to approximate the various shapes of specific detectivity curves in different spectral domains. Moreover, the effect of the chosen spectral band and the change of the NETD inside the whole spectral domain are studied taking into account two cases: overlapping subintervals and non-overlapping subintervals.

*Keywords:* thermal imager, thermal sensitivity, thermal noise, mathematical model, parameter analysis.

### Introduction

#### *Evaluating the performance of thermal imagers*

IN order to evaluate the performance of thermal imagers, thermal imager specification parameters are selected to provide a relatively simple way to quantify the image quality and sensitivity limits. They could be used for measurement results correction, or the prediction of the performance limits in their field of application. This is crucial for correct temperature measurements and results interpretation as well as for taking corrective actions.

These parameters can be classified into two groups: objective and subjective parameters [1]. Any system using a thermal camera for practical purposes requires a combination of these two groups of parameters to describe its performance.

Subjective parameters such as MRTD (Minimum Resolvable Temperature Difference) and MDTD (Minimum Detectable Temperature Difference) take essentially into account the display performances and the perception limits of a subjective observer (human eye). They have a significant importance for observers who seek the highest range of detection, recognition and identification of specific targets [2].

Objective or accuracy parameters such as NETD (Noise Equivalent Temperature Difference) and IFOV (Instantaneous Field Of View) are necessary to evaluate thermal

imagers which are used as non-contact thermometers. However, they are less useful for thermal cameras used in surveillance systems [3–5].

#### *Noise sources in thermal imagers*

The central function of infrared cameras for the army is the detection and recognition of desired images, soldiers, fixed and mobile military equipment in the presence of spatial clutter: grass, trees, rocks, civilian cars, trucks, etc. Camera noise and nonuniformity also produce a type of clutter [3], [6]. The push towards larger detector arrays with more pixels in recent years has been driven by the realization that many pixels on target are needed to separate important images from clutter, to identify the target and to distinguish a friend from a foe [3].

In general, images generated by infrared systems are low in contrast and are sensitive to any kind of noise. Infrared systems suffer from mainly two types of noise: temporal noise and spatial noise. For the separation of images from clutter, the spatial characteristics of the image and the detector array are as important as the temporal characteristics [3].

Temporal noise changes from one frame to another and is caused by:

- Dark current shot noise due to thermally generated charge carriers,

<sup>1)</sup> University of Defense, Military Academy, Generala Pavla Jurišića Šturma 33, 11000 Belgrade, SERBIA

<sup>2)</sup> Military Technical Institute (VTI), Ratka Resanovića 1, 11132 Belgrade, SERBIA

<sup>3)</sup> Teleoptik žiroskopi, Filipa Fišnjića 31, 11080 Zemun, SERBIA

<sup>4)</sup> University of Belgrade, Institute of Physics, Prigrevica 118, 11080 Zemun, SERBIA

- Electronic noise such as 1/f noise, thermal noise and reset noise.

Spatial noise is more or less static between frames. It can be seen as a fixed pattern in each frame and is usually referred to as Fixed Pattern Noise (FPN). FPN is the dominant noise source in most staring infrared systems. The main reason for FPN is imperfections in the detectors. Each detector can show significant differences in responsivity, gain, and noise. A non-uniformity correction (NUC) process can efficiently cancel out FPN [7].

The examples of two common types of noise are shown in Fig.1-a and 1-b [5].

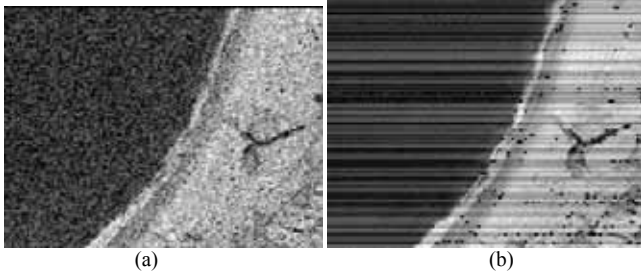


Figure 1. (a) Temporal Noise; (b) Fixed Pattern Noise.

### Noise equivalent temperature difference concept

NETD is defined as the temperature difference between a test target and the background that produces a signal equivalent to the (temporal) noise [1], [8], [9]. It is also called by some manufacturers: “thermal sensitivity”, “thermal resolution” or “temperature resolution” but usually means the noise equivalent temperature difference which provides information about the noise that affects a thermal imager and which limits the smallest temperature difference that could be detected.

When an infrared signal is affected by noise, once it is converted to an image depicting temperatures, the noise can be measured in terms of temperature (in degrees). It is very important to know this level of noise, since it causes a variation in temperature that is not due to the target situated in the field of view. To illustrate this concept, Fig.2 depicts the variation in time of measured temperatures for one pixel during 20 seconds [1]. As it can be seen, there are always small variations in temperature which are assumed not to be caused by the considered target.

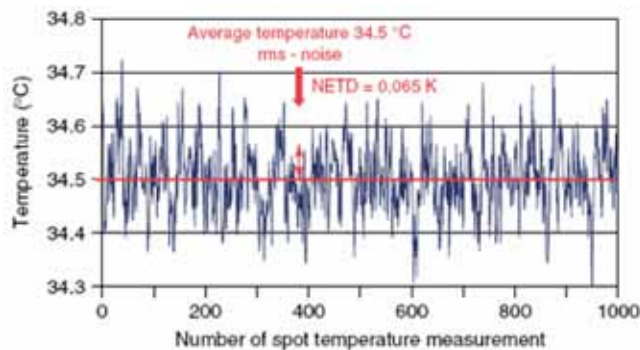


Figure 2. Time dependence of spot temperatures.

The frequency distribution of the measured spot temperatures can be approximated by a standardized normal distribution, as expected for random noise processes (Fig.3). The experimental NETD represents the half-width of the standardized normal distribution [1].

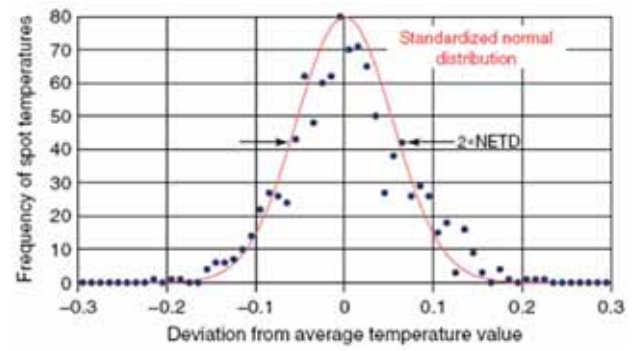


Figure 3. Frequency distribution of the measured spot temperatures centred around the average temperature.

NETD is limited in that it only characterizes the detector temporal noise [2], [8]. Furthermore, NETD is strongly dependent on the temperature that dominates the scene (as explained in [10]) and the cut-off wavelength (as explained in [11]). It does not take into account the whole electronic system, the display, or the observer and it is also independent of the spatial frequency, therefore it is not taken as a parameter to measure the overall quality of thermal imagers [2].

### Mathematical model

In this paper, one of the most used and most appropriate forms for determining NETD is chosen, which takes into consideration almost all the parameters of an infrared camera [4], [5], [8], [12–18].

The eq. describing NETD can be carried out starting from the spectral irradiance at a given aperture:

$$E_{e\lambda ap} = \frac{M_{e\lambda}}{\pi} \cdot \frac{A_0}{R^2} \cdot \tau_a(\lambda), \quad (1)$$

where:

$A_0$  [cm<sup>2</sup>]: The objective's area,

$R$  [km]: The distance from the source of infrared radiation (observation range),

$\tau_a$ : Transmission in the atmosphere which is given by Beer Law:

$$\tau_a = e^{-\sigma R}, \quad (2)$$

$\sigma$  [km<sup>-1</sup>]: Extinction coefficient,

$M_{e\lambda}$  [W/m<sup>2</sup>] $\mu$ m: Spectral exitance, defined as:

$$M_{e\lambda}(\lambda) = \frac{c_1}{\lambda^5} \left[ \frac{1}{e^{\frac{c_2}{\lambda T}} - 1} \right], \quad (3)$$

where  $c_1$  and  $c_2$  are the first and the second radiation constants, respectively:

$$c_1 \left[ \text{W}\mu\text{m}^4/\text{cm}^2 \right] = (3.741832 \pm 0.000020) \cdot 10^4,$$

$$c_2 \left[ \mu\text{m K} \right] = (1.438786 \pm 0.000045) \cdot 10^4.$$

The incident flux at the detector is:

$$\phi_{e\lambda} = E_{e\lambda ap} \omega R^2 \tau_0(\lambda), \quad (4)$$

i.e.:

$$\phi_{e\lambda} = \frac{M_{e\lambda}}{\pi} \omega A_0 \tau_a(\lambda) \tau_0(\lambda), \quad (5)$$

where:

$\omega$ [sr]: The solid angle covering the actual field of view,

$\tau_0$ : Transmission of the optical system.

It is considered that the target spectral radiance corresponds to the spectral radiance of an absolute black body: This means that the product of the target emissivity and spectral radiance is equivalent to the radiance of an ideal black body:

$$\varepsilon_T(\lambda, T_T) \cdot L_{e\lambda}(\lambda, T_T) = L_{e\lambda}(\lambda, T_T) = L_{e\lambda}, \quad (6)$$

$\varepsilon_T$ : The target emissivity,

$T_T$ [K]: The target temperature,

$L_{e\lambda}(\lambda, T_T)$ [W/m<sup>2</sup>sr $\mu$ m]: The spectral radiance of the target,

$L_{e\lambda}^*(\lambda, T_{BB})$ [W/m<sup>2</sup>sr $\mu$ m]: The spectral radiance of an absolute black body,

Bearing in mind that:

$$\Delta M_{e\lambda} = M_{e\lambda T} - M_{e\lambda B} = M_{e\lambda}(T_B + \Delta T, \lambda) - M_{e\lambda}(T_B, \lambda), \quad (7)$$

where:

$M_{e\lambda T}$  [W/m<sup>2</sup> $\mu$ m]: The target spectral exitance,

$M_{e\lambda B}$  [W/m<sup>2</sup> $\mu$ m]: The background spectral exitance,

$T_B$ [K]: The background temperature.

The variation of the incident flux with the temperature is:

$$\frac{\partial \phi_{e\lambda}}{\partial T} = \frac{\partial M_{e\lambda}}{\partial T} \frac{\omega}{\pi} A_0 \tau_a(\lambda) \tau_0(\lambda), \quad (8)$$

The response relative to the incident flux is defined as

$$R_0 = \frac{V_S}{\phi_{e\lambda}},$$

where:

$V_S$ [V]: The mean square value of the voltage signal at the detector output.

So the variations of  $V_S$  with the temperature  $T$  could be written as:

$$\frac{\partial(\delta V_S)}{\partial T} = \frac{\omega}{\pi} A_0 \tau_a(\lambda) \tau_0(\lambda) R_0(\lambda) \frac{\partial M_{e\lambda}}{\partial T}. \quad (9)$$

The response can be also defined as:

$$R_0 = \frac{V_N}{NEP(\lambda)} = V_N D(\lambda) = \frac{V_N D^*(\lambda)}{\sqrt{A_D \Delta f_N}}, \quad (10)$$

where:

$NEP(\lambda)$ [W]: Noise equivalent power, which is defined as the amount of incident flux at which the signal to noise ratio is equal to unity (SNR=1),

$D^*(\lambda)$ [cm $\sqrt$ Hz)/W]: Spectral specific detectivity,

$A_D$ [cm<sup>2</sup>]: The area of each detector's element,

$V_N$ [V]: The mean square value of the voltage signal at the detector output,

$\Delta f_N$ : The noise bandwidth.

The replacement of  $R_0$  in eq.9 gives:

$$\frac{\partial(\delta V_S)}{\partial T} = \frac{\omega}{\pi} A_0 \tau_a(\lambda) \tau_0(\lambda) \frac{V_N D^*(\lambda)}{\sqrt{A_D \Delta f_N}} \frac{\partial M_{e\lambda}}{\partial T}, \quad (11)$$

By the integration of eq.11 and applying the approximation for small signals, the following form is obtained:

$$\frac{\partial V_S}{\partial T} \cong \frac{\Delta V_S}{\Delta T} = \frac{\omega A_0 V_N}{\pi \sqrt{A_D \Delta f_N}} \int_0^\infty \frac{\partial M_{e\lambda}}{\partial T} D^*(\lambda) \tau_a(\lambda) \tau_0(\lambda) d\lambda. \quad (12)$$

i.e.:

$$\frac{\Delta V_S}{V_N} = \Delta T \frac{\omega A_0}{\pi \sqrt{A_D \Delta f_N}} \int_0^\infty \frac{\partial M_{e\lambda}}{\partial T} D^*(\lambda) \tau_a(\lambda) \tau_0(\lambda) d\lambda. \quad (13)$$

In the case where the condition  $\Delta V_S / V_N = 1$  is fulfilled, the variation  $\Delta T$  will match the NETD, i.e.  $\Delta T$ [K]  $\equiv$  NETD [K], so that eq.13 becomes:

$$NETD = \frac{\pi \sqrt{A_D \Delta f_N}}{\omega A_0 \int_0^\infty \frac{\partial M_{e\lambda}}{\partial T} D^*(\lambda) \tau_a(\lambda) \tau_0(\lambda) d\lambda} \quad (14)$$

In practice, the temperature difference of two sources, which can be considered as two black bodies that completely close the inlet of an infrared optical system, will correspond to the NETD if the difference of the mean square values of the signal equals to the mean square value of the noise.

The effective values of the transmissions  $\tau_0$  and  $\tau_a$  are constant inside the work range  $\lambda_1 \leq \lambda \leq \lambda_2$  and zero outside this range:

$$\tau_a \tau_0 = \frac{\int_0^\infty \frac{\partial M_{e\lambda}(T_B)}{\partial T} D^*(\lambda) \tau_a(\lambda) \tau_0(\lambda) d\lambda}{\int_0^\infty \frac{\partial M_{e\lambda}(T_B)}{\partial T} D^*(\lambda) d\lambda}. \quad (15)$$

In addition, the ratio of the specific detectivity  $D^*(\lambda)$  and the peak detectivity is called the detector relative detectivity  $D_{rel}^*(\lambda)$ . Multiplying and dividing by the detector peak detectivity  $D_{\lambda_p}^* = D^*(\lambda_2)$ , allows obtaining a normalized integral. The normalized value of the integral represents the variation of the effective spectral exitance with the temperature:

$$\frac{\Delta M_e}{\Delta T} \cong \int_{\lambda_1}^{\lambda_2} \frac{\partial M_{e\lambda}(T_B)}{\partial T} \frac{D^*(\lambda)}{D_{\lambda_p}^*} d\lambda. \quad (16)$$

The partial derivative of  $M_{e\lambda}$  with the respect to  $T$  is:

$$\frac{\partial M_{e\lambda}}{\partial T} = \frac{c_2}{\lambda T_B^2} M_{e\lambda}(T_B). \quad (17)$$

Applying this approximation to eq.14, it takes the form:

$$NETD = \frac{\pi \sqrt{A_D} \Delta f_N}{\omega A_0 \tau_a \tau_0 D_{\lambda_p}^* \frac{c_2}{T_B^2} \int_{\lambda_1}^{\lambda_2} \frac{\partial M_{e\lambda}(T_B)}{\partial T} \frac{D^*(\lambda)}{D_{\lambda_p}^*} d\lambda} \quad (18)$$

After we substitute:

$$A_0 = D_{tu}^2 \frac{\pi}{4}, \quad \Delta f_N = \frac{\pi}{2} \cdot \frac{1}{2\tau_d}, \quad n_{pl} = \frac{\theta_H}{\alpha_D^H}, \quad n_l = \frac{\theta_V}{\alpha_D^V},$$

$$N_{ps} = n_l n_{pl},$$

$$\tau_d = \frac{N \cdot \alpha_D^H \cdot \alpha_D^V \cdot \rho \cdot p_l}{\theta_H \cdot \theta_V \cdot F_R \cdot \eta} = \frac{n_s \cdot n_p \cdot \rho \cdot p_l}{n_l \cdot n_{pl} \cdot F_R \cdot \eta} = \frac{n_s \cdot n_p \cdot \rho \cdot p_l}{N_{ps} \cdot F_R \cdot \eta},$$

$$\omega = \frac{A_D}{f_0^2}, \quad F\# = \frac{f_0}{D_{tu}} = \frac{1}{2NA},$$

the last eq. for the NETD takes the form [8–14], [19]:

$$NETD = \frac{2\sqrt{\pi} (F\#)^2}{\sqrt{A_D} \cdot \tau_0 \cdot \tau_a \cdot D_{\lambda_p}^* \cdot \int_{\lambda_1}^{\lambda_2} \frac{\partial M_{e\lambda}}{\partial T} \frac{D^*(\lambda)}{D_{\lambda_p}^*} d\lambda} \cdot \sqrt{\frac{N_{ps} \cdot F_R \cdot \eta}{n_s \cdot n_p \cdot \rho \cdot p_l}}, \quad (19)$$

where:

- $F\#$ : The  $f$ -number,
- $f_0$  [mm]: The objective focal length,
- $D_{tu}$  [mm]: The objective diameter,
- $N_{ps}$ : The number of infrared pixels in one image,
- $n_l$ : The number of infrared lines in one picture,
- $n_{pl}$ : The number of pixels in one line,
- $\theta_V$ : The vertical field of view,
- $\theta_H$ : The horizontal field of view,
- $\alpha_D^V$ : The vertical vision angle of the instantaneous field of view,
- $\alpha_D^H$ : The horizontal vision angle of the instantaneous field of view,
- $[\lambda_1, \lambda_2]$ : The spectral range,

- $F_R$ : The frame rate,
- $n_p$ : The number of parallel detectors,
- $n_s$ : The numbers of serial detectors,
- $\rho$ : Scanning efficiency coefficient,
- $\eta$ : Lines insertion coefficient (interlace),
- $p_l$ : Lines overlapping coefficient.

As it can be seen from the chosen model above, the NETD is influenced by the camera's optics and all attenuation factors that affect the incident radiation (transmittance of the atmosphere, the optics, etc.) as well as the characteristics of the detector. The detector is assumed to receive a certain amount of radiation within the considered wavelength region  $\lambda_1 \leq \lambda \leq \lambda_2$ . The specific detectivity  $D^*$ , which is one of the most important characteristics of a detector, depends on the wavelength [8].

The mathematical model in eq.19 is supposed to estimate the NETD of thermal imagers with opto-mechanical scanning (1<sup>st</sup> and 2<sup>nd</sup> generation). Its upgraded version that is able to estimate the NETD of thermal imagers known as 3<sup>rd</sup> generation, staring or Focal Plane Array thermal imagers introduces a parameter named fill factor ( $ff$ ), so that eq.19 becomes:

$$NETD = \frac{2\sqrt{\pi} (F\#)^2}{\sqrt{A_D} \cdot \tau_0 \cdot \tau_a \cdot D_{\lambda_p}^* \cdot \int_{\lambda_1}^{\lambda_2} \frac{\partial M_{e\lambda}}{\partial T} \frac{D^*(\lambda)}{D_{\lambda_p}^*} d\lambda} \sqrt{F_R \cdot ff} \quad (20)$$

The fill factor is the ratio of the active detector area and the total detector area. The fill factor determines the maximum achievable sensitivity [20] (see Fig.4 [1]) i.e. it determines the NETD.

For square shaped detector elements, the fill factor ( $ff$ ) is given as:

$$ff = \frac{A_D}{pitch^2}, \quad (21)$$

where the pitch is the distance between the centres of the adjacent detector elements.

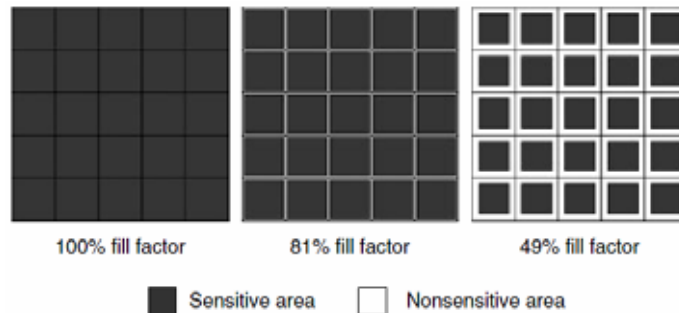


Figure 4. Fill factor of an FPA.

### Numerical model

In order to evaluate the performance of several types of thermal imagers, the mathematical NETD model, explained in the previous section, was implemented on a suitable software package for mathematical modelling and graphical user interface in order to see the effect of each parameter on the overall NETD value.

As it is known, the figure of merit for radiation detectors is the value of  $D^*(\lambda)$  [1]. According to the latter, the performance of all different radiation detectors can be compared (see Fig.5 [21]). The knowledge of the trend of  $D^*(\lambda)$ , for a given detector material and a bandwidth, allows the estimation of the appropriate noise equivalent temperature difference.

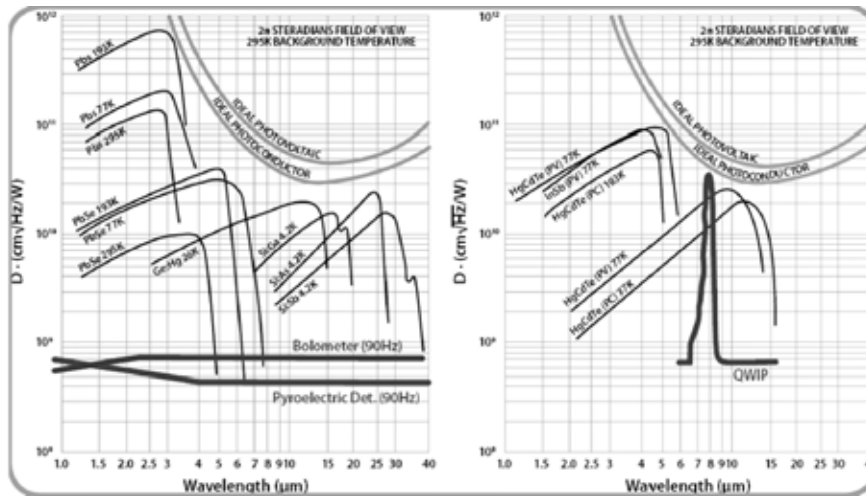


Figure 5. Spectral specific detectivity curves ( $D^*$ ) for different detector materials.

The spectral range of interest is usually between 3 and 5  $\mu\text{m}$  or between 8 and 14  $\mu\text{m}$ . For this reason, and taking into account the data provided by the manufacturers (see Fig.5), the variation of spectral specific detectivity for the estimation of the NETD in the interval of interest can be considered as one of the following models [5], [18], [22-23]:

Constant:  $D^*(\lambda) = D_{\lambda_p}^*$

Linear:  $D^*(\lambda) = a\lambda + b$

Logarithmic:  $D^*(\lambda) = a \ln(\lambda) + b$

Parabola:  $D^*(\lambda) = a(\lambda - \lambda_0)^2 + D_{\lambda_p}^*$

Where  $\begin{cases} a > 0 \\ \lambda_0 = \frac{\lambda_1 + \lambda_2}{2} \end{cases}$

Ramp:  $\begin{cases} D^*(\lambda) = D_{\lambda_p}^* & \text{for } \lambda \leq \lambda_0 \\ D^*(\lambda) = a\lambda + b & \text{for } \lambda > \lambda_0 \\ \lambda_0 = \frac{\lambda_1 + \lambda_2}{2} \end{cases}$

To facilitate the task for the user, a graphical interface is developed and is organised in a very simple way to help any operator to calculate the NETD for a certain number of cameras, using the model mentioned above. After that, the

obtained results could be easily compared with the values given by the producer [4], [5], [22 – 24].

First, users have to enter all the parameters related to the device in question which are necessary for the calculation. Then they must choose one of the available models that approximate the spectral specific detectivity. This choice must be done in accordance with the wavelength range and the curves given by the manufacturer for different detector materials (see Fig.5). After that, they have the possibility to choose between two types of thermal cameras: thermal cameras with optomechanical scanning (the first and the second generation) or thermal cameras with Focal Plane Array (the third generation). The choice is achieved by clicking on one of the two specific buttons. In the case of choosing thermal cameras with a focal plane array, two new windows appear and the number of horizontal and vertical detectors must be entered, whereas when choosing the first and the second generation, other parameters should be specified (see Eq. 19): the number of infrared lines in one picture, the number of pixels in one line, scanning efficiency coefficient, lines overlapping coefficient, lines overlapping coefficient and lines insertion coefficient (interlace).

Finally, the interface will allow the user to read immediately the horizontal and vertical field of view and the calculated NETD value (as shown in Fig.6).

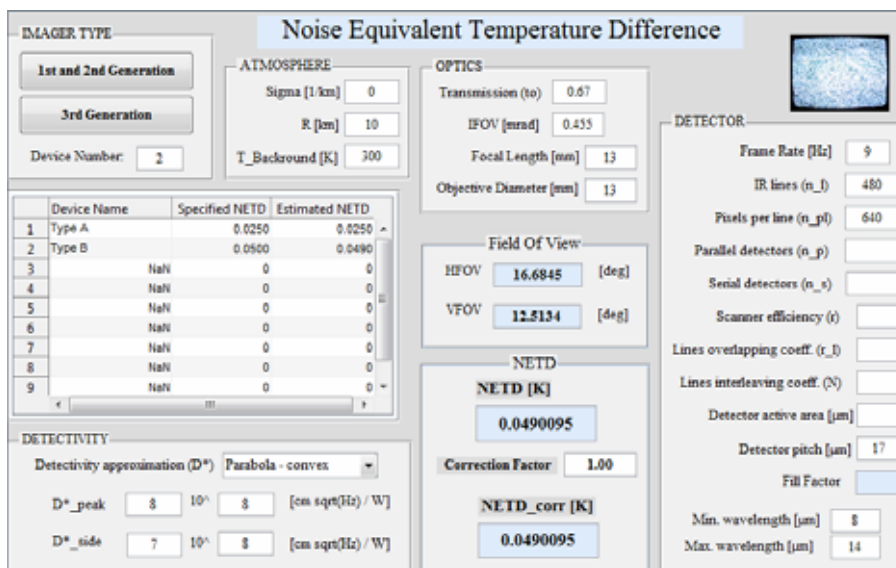


Figure 6. Graphical user interface for calculating the NETD.

In the case of checking more than one device, the users can prepare a table shown below (Table 1) in a specific Excel file. After that, the number of each camera should be entered in the interface as well as the rest of the parameters specified before. At the end of each NETD calculation for each camera, its value will be saved automatically in the Excel file. Finally, the declared NETD value, which has to be filled by the user, could be easily compared with the one calculated with this model.

**Table 1.** The table in the Excel file prepared for NETD estimation.

	Device Name	Specified NETD [K]	Estimated NETD [K]
1	FLIR SC7000 Series	0.025	
2	Electrophysics PV640LW	0.050	
3	CMC Electronics Cincinnati NC256	0.040	
4	Irvine Sensors Inc	0.080	

Furthermore, another numerical simulation is performed to observe the effect of the chosen spectral range on the value of the estimated NETD, as well as the trend of the NETD inside the whole spectral domain.

The aim of this part is to conclude later on the effect of using one detector with a large spectral range, or a multiple number of detectors with a relatively narrow spectral range, on the NETD value.

For this reason, the whole spectral range was divided into  $N$  subintervals and the NETD value was calculated inside each subinterval taking into account two following cases;

- The subintervals are adjacent and do not overlap.
- The subintervals overlap.

## Results and discussion

In order to check the validity of this model, NETD is estimated using our considered model for different thermal cameras. Then, the obtained values are compared with the ones specified by different producers. The obtained results, as well as the values provided by the manufacturers [25–28] are summarized in Table 2.

**Table 2.** NETD estimated for different thermal cameras.

Types of IR cameras	CMC Electronics Cincinnati Night Conquerer Flir Receiver	FLIR SC7000 Series	Electrophysics PV640LW	Irvine Sensors Inc
Spectral Band [ $\mu\text{m}$ ]	3.6 - 5.0	3.7 - 4.8	8 - 14	8 - 12
Resolution [pixels]	640 x 512	320 x 256	640 x 480	640 x 480
Pitch [ $\mu\text{m}$ ]	28	30	17	25
F-number	f/4	f/3	f/1	f/1.25
Wide FOV	21.2° x 15.9°	22° x 17°	45°	24.6° x 32.7°
Focal length [mm]	48	25	50	28.4
Narrow FOV	3.0° x 2.3°	2.75° x 2.2°	12.5°	/
Focal length [mm]	342	200	13	/
Frame Rate [Hz]	25	25	60	30
Specified NETD @ 25°C [mK]	< 40	< 25	< 50	< 80
Estimated NETD [mK]	44.62	26.96	56.12	87.09

It can be clearly seen from the previous table (Table 2) that the values given by producers are in harmony to a certain extent with the values calculated using the mentioned model.

The results obtained when varying the number of

subintervals to calculate the NETD for the FLIR SC7000 Series thermal camera are illustrated in Fig. 7, where  $N$  is the number of non-overlapping subintervals and  $L$  is the spectral width of each overlapping subinterval.

Overall, it can be clearly noticed that the NETD value increases with the increase in the number of subintervals. Besides, the NETD value is bigger for the small values of the wavelength and decreases with the increase in its value.

In addition, it is noticed that the overlapping between the subintervals has no noticeable effect on the NETD value and its general trend.

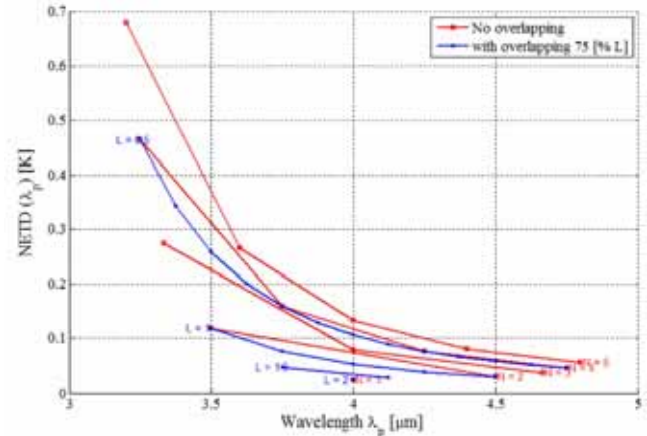


**Figure 7.** The effect of the chosen spectral range on the NETD value.

## Conclusion

From a closer analysis of the obtained results, it is concluded that the proposed model can be efficiently used to estimate the NETD of a various number of thermal imagers in a more practical way. In fact, it is very useful to know NETD, not only as a performance parameter in itself, but also as an important variable to determine other parameters that assess the performance and the quality of any thermal imager, the MRTD for example. Besides, using this simulation model makes the process much easier and quicker.

The model from Eq. 19 was used in the first place for thermal imagers with an opto-mechanical scanning system, whereas the presented model is upgraded to be able to estimate the NETD of thermal cameras with a focal plan array.

Moreover, it is demonstrated that the chosen spectral interval has a big effect on the NETD value. In fact, using a big number of subintervals increases the NETD value, which deteriorates the performance of any chosen infrared camera. This could be explained by the fact that the chosen mathematical model in this paper is strongly dependent on the considered spectral interval, and by taking a big number of subintervals, this means narrowing the limits in the integral (in Eq. 19), which increases NETD.

In conclusion, from the previous study on the effect of spectral subintervals, it can be generally said that using one detector with a large spectral band is far better than using a big number of detectors with a relatively narrow spectral band for any given thermal imager.

## Acknowledgments

This work was supported by the Military Technical Institute in Belgrade, the Laboratory of Optoelectronics.

Darko Vasiljevic would also like to acknowledge Grant

No.III45016 (2011. – 2014.) financed by the Ministry of Education, Science and Technological Development of the Republic of Serbia.

## References

- [1] VOLLMER,M.,L MÖLLMANN,K.P.: *Infrared Thermal Imaging Fundamentals, Research and Applications*, Wiley-VCH Verlag GmbH & Co,Weinheim, Germany, 2010.
- [2] CHRZANOWSKI,K.: *Testing Thermal Imagers Practical Guidebook*, Military University of Technology, 00-9085, Warsaw, Poland, 2010.
- [3] WESTERVELT,R., ABARBANEL,H., GARWIN,R., JEANLOZ,R., Kimbel,J., SULLIVAN,J., WILLIAMS,E.: *Imaging Infrared Detectors II*, Jason, the MITRE Corporation, 1820 Dolley Madison Boulevard, Mclean, Virginia, October 2000, 22102-3481.
- [4] MOYER,S.K.: *Modeling Challenges of Advanced Thermal Imagers*, Dissertation presented in partial fulfillment of the requirements for the degree of PhD in Electrical Engineering, Academic Faculty, Georgia Institute of Technology, August 2006.
- [5] US Army Night Vision and Electronic Sensors Directorate, Modeling & Simulation Division, "User's Manual & Reference Guide, Night Vision Thermal Imaging Systems Performance Model", Document: Rev 5, Fort Belvoir, VA, March 12, 2001.
- [6] NIKLAUS,F., JANSSON,C., DECHARAT,A., KÄLLHAMMER,J.E., PETTERSSON,H., STEMME,G.: *Uncooled Infrared Bolometer Arrays Operating in a Low to Medium Vacuum Atmosphere: Performance Model and Tradeoffs*, SPIE Conference, Infrared Technology and Applications XXXIII, Orlando, USA 2007.
- [7] ACCETTA,J.S., SHUMAKER,D.L., DUDZIK,M.C.: *The Infrared and Electro-Optical Systems Handbook*, Volume 4, Electro-Optical Systems Design, Analysis, and Testing, Copublished by Infrared Information Analysis Center, Environmental Research Institute of Michigan, Ann Arbor, Michigan USA, and SPIE Optical Engineering Press, Bellingham, Washington USA, 1994.
- [8] North Atlantic Treaty Organisation, *Experimental Assessment Parameters and Procedures for Characterisation of Advanced Thermal Imagers*, RTO Technical Report 75 (II), 2003.
- [9] ASTM Committee E07 on Nondestructive Testing, *Standard Test Method for Noise Equivalent Temperature Difference of Thermal Imaging Systems*, Designation: E1543-00, Reapproved December 2011, Published March 2012.
- [10] LHUILLIERE., MOHAMED,I.R., LAPERNE,N.P., TAUUVY,M., DESCHAMPS,J., NEDELUCU,A., ROSENCHER,E.: *15  $\mu$ m Quantum Well Infrared Photodetector for Thermometric Imagery in Cryogenic Windtunnel"*.
- [11] VOITSEKHOVSKII,A.V., KOKHANENKO,A.P., NESMELOV,S.N.: *Spectral Detectivity and NETD of Doping-Spike Ptsi/p-Si and Gesi/Si HIP Detectors*, Opto-Electronics Review, 2003, 11(2), pp.161-167.
- [12] LIVADA,B.: *Mogućnosti protivelektronskog obezbeđenja u oblasti primene termovizijskih uređaja i sistema'*, internal document, VTI 019-11.0158, Beograd, 1994.
- [13] PECOTIC,N.: *Uvod u projektovanje sistema'*, internal document, VTI 03-27-26, 1981.
- [14] UGARTE,A.R.: *Modelling For Improved Minimum Resolvable Temperature Difference Measurements'*, PhD dissertation, Naval Postgraduate School, Monterey, California, September 1991.
- [15] HUDSON,R.D.jr.: *Infrared System Engeneering*, New York / London / Sydney / Toronto, John Wiley & Sons. Inc, 1969.
- [16] KNEŽEVIĆ,D.: *Analiza termovizijskih uređaja za detekciju ciljeva u vazduhu*, Magistarska teza, Elektrotehnicki fakultet, Univerziteta u Beogradu, 2001.
- [17] LOYD,J.M.: *Thermal imaging System*, Plenum Press, New York, 1975.
- [18] ROGALSKI,A.: *Infrared Detectors for the Future*, Optical and Acoustical Methods in Science and Technology, ACTA PHYSICA POLONICA A, 2009, Vol.116, No.3.
- [19] RATCHES,J.A. et al: *Night Vision Laboratory Static Performance Model for Thermal Viewing Systems*, Army Electronics Comand, Fort Monmount, New Jersey, NTIS AD-A/011212, April 1975.
- [20] BLANC,N.: *CCD versus CMOS - has CCD imaging come to an end?*, Photogrammetric Week 2001, D. Fritsch and R. Spiller (Eds.), Institut für Photogrammetrie , Stuttgart, Germany, 2001.
- [21] FLIR Systems, *The Ultimate Infrared Handbook for R&D Professionals*, 2014, www.flir.com.
- [22] ROGALSKI,A.: *Infrared Detectors: Status and Trends*, Progress in Quantum Electronics Review 2003, 27, pp.59-210.
- [23] Kozlowski,L.J., Kosonocky,W.F.: *Infrared Detector Arrays*, Chapter 23.
- [24] ROSU,I.: *Understanding Noise Figure*, YO3DAC / VA3IUL, http://www.qsl.net/va3iul.
- [25] FLIR Systems, *Advanced Thermal Imager Cameras for R&D and Science Applications*, December 2011, http://www.flir.com/uploadedFiles/Thermography/MMC/Brochures/T820168/T820168\_APAC.pdf.
- [26] SOFRADIR EC (formerly Electrophysics Thermal Imaging Cameras), *Technical Characteristics of Uncooled Thermal Camera PV640LW*, Fairfield, USA, 2013, http://www.tlsbv.nl/pages/downloads/2013/Sofradir/Sofradir%20EC%20PV640%20Brochure.pdf
- [27] THEURER,L.: *Evaluation of Modulation Transfer Function Algorithms*, Chapter 2, Page 11, September 10, 2012.
- [28] Cincinnati Electronics, *Specifications of NightConqueror Flir Receiver*, Infrared Products, 7500 Innovation Way, Mason, Ohio, September 12, 2005, www.L-3com/CE.

Received: 18.03.2014.

## Modelovanje temperaturske razlike ekvivalentne šumu kod termalnih kamera, proračun i analiza

Smatra se da temperaturska razlika ekvivalentna šumu (NETD) ili termička osetljivost ima veliku važnost za proces vrednovanja i upoređivanja performansi termovizijskih kamera koje su u suštini uređaji za beskontaktno merenje temperature. Ovaj rad opisuje aplikaciju za proračun NETD-a zasnovan na specifičnoj detektivnosti detektora. NETD nekoliko termalnih kamera je procenjen i upoređen sa vrednostima koje su deklarisali proizvođači. Matematički model korišćen u ovom procesu se veoma oslanja na specifičnu detektivnost detektora. Zbog toga je uveden određen broj geometrijskih krivih za aproksimaciju oblika krivih specifične detektivnosti u različitim spektralnim opsezima. Osim toga, razmatrani su uticaj odabranog spektralnog opsega i promena NETD-a uzimajući u obzir dva slučaja: preklapljen podopsege i nepreklapljen podopsege.

*Cljučne reči:* termovizijska kamera, termička osetljivost, termički šum, matematički model, analiza parametara.

## **Modélisation de la température équivalente du bruit de caméras thermiques, calcul et analyse**

La température équivalente du bruit ou la sensibilité thermique (NETD) a une importance significative dans le processus d'évaluation et de la comparaison des performances des caméras thermiques et qui sont en réalité des dispositifs de mesure sans contact de la température. Cet article décrit une application pour le calcul du NETD basée sur la détectivité spécifique du détecteur. Le NETD a été estimé pour plusieurs types de caméras thermiques et comparé ensuite avec les valeurs déclarées par les producteurs. Le modèle mathématique utilisé dépend fortement de la détectivité spécifique du détecteur. Pour cette raison un certain nombre de modèles géométriques décrivant la détectivité spécifique sont introduits pour différents domaines spectraux. En plus l'effet de l'intervalle spectral choisi et la tendance du NETD à l'intérieur du domaine spectral global sont étudiés en tenant en considération deux cas possibles : des sous-intervalles qui chevauchent entre eux ainsi que des sous-intervalles séparés.

*Mots clés:* caméra thermique, sensibilité thermique, bruit thermique, modèle mathématique, analyse des paramètres

## **Modélisation de la temperature equivalente du bruit des cameras thermiques, calcul et analyse**

La température équivalente du bruit ou la sensibilité thermique (NETD) a une importance significative dans le processus d'évaluation et de la comparaison des performances des caméras thermiques et qui sont en réalité des dispositifs de mesure, sans contact, de la température. Cet article décrit une application pour le calcul du NETD basée sur la détectivité spécifique du détecteur. Le NETD a été estimé pour plusieurs types de caméras thermiques et comparé ensuite avec les valeurs déclarées par les producteurs. Le modèle mathématique utilisé dépend fortement de la détectivité spécifique du détecteur. Pour cette raison, un certain nombre de modèles géométriques, décrivant la détectivité spécifique, sont introduits pour différents domaines spectraux. En plus, l'effet de l'intervalle spectral choisi et la tendance du NETD à l'intérieur du domaine spectral global sont étudiés, en tenant en considération deux cas possibles: des sous-intervalles qui chevauchent entre eux ainsi que des sous-intervalles séparés.

*Mots clés:* température équivalente du bruit, détectivité spécifique, caméras thermiques, la sensibilité thermique, facteur de remplissage.